10.2478/v10160-012-0024-4

Transactions of the VŠB – Technical University of Ostrava

No. 2, 2012, Vol. XII, Civil Engineering Series

paper #20

Mária MINÁROVÁ[1], Jozef SUMEC[2], Mária TJEŠŠOVÁ[3]

BEHAVIOR OF THE INTERVERTEBRAL DISC WITHIN THE MOTION SEGMENT L3-L4 OF THE HUMAN SPINE UNDER VARIOUS TYPES OF PHYSIOLOGICAL LOAD

ODOZVA MEDZISTAVCOVEJ PLATNIČKY V RÁMCI POHYBOVÉHO SEGMENTU L3-L4 ĽUDSKEJ CHRBTICE NA RÔZNE TYPY FYZIOLOGICKÉHO ZAŤAŽENIA

Abstract

The paper deals with the biomechanical investigation on the motion segment – basic part of the human lumbar spine focused on the intervertebral disc response to the various types of load. It contains the description and the reason of the simplification of the model, the biomechanical laws; the mathematical treatment with the computational implementation added. The results are presented and discussed especially for the intervertebral disc.

Keywords

Lumbar spine, motion segment, intervertebral disc, equilibrium equations in cylindrical system of coordinates, finite element analysis.

Abstrakt

Článok sa zoberá skúmaním reakcie pohybového segmentu ľudskej chrbtice na rôzne druhy zaťaženia. Zameriava sa prioritne na odozvu medzistavcovej platničky na tieto zaťaženia. Popisuje geometriu zjednodušeného modelu pohybového segmentu spolu s odôvodnením tohto zjednodušenia, biomechanické zákony, matematický model popisujúci fyzikálny dej. Načrtáva konečno prvkovú analýzu, podáva a analyzuje výsledky počítačovej implementácie.

Kľúčové slová

Lumbálna chrbtica, pohybový segment, medzistavcová platnička, rovnice rovnováhy v cylindrických súradniciach, konečno prvková analýza.

1 INTRODUCTION

Human lumbar spine diseases become more and more frequent in nowadays generation. The pain in this part of the spine very often restricts or disables the afflicted person in his work activity or even in the common life. The most often cause of the low back pain onset is the intervertebral disc degeneration. There are several reasons of this pathology, as wrong body control, injury, the overload at work - persisting in the same posture for a long time, heavy physical work, frequent repeating motions as lifting or bending, vibrations, etc. As the treatment of the patient with such a diagnosis is

[1] RNDr. Mária Minárová, PhD.,Slovak Technical University, Faculty of Civil Engineering, Dpt. of Mathematics, Radlinského 11, 81368 Bratislava, tel.: +421 59274 236, e-mail: minarova@math.sk

[2] Prof. Ing. RNDr. Mgr. Jozef Sumec, DrSc., Slovak Technical University, Faculty of Civil Engineering, Dpt. of Structural Mechanics, Radlinského 11, 81368 Bratislava, tel.: +421 59274 455, e-mail: jozef.sumec@stuba.sk

[3] Mária Tješšová, student, Slovak Technical University, Faculty of Civil Engineering, Radlinského 11, 81368 Bratislava, e-mail: maria.tjessova@gmail.com

often invasive (the X-rays side effect to human organism is well known), costly and long-lasting, the theoretical investigation in this field is unavoidable. And this is the task for biomechanics.

In this paper there is a simplified model of human spine motion segment described. The motion segment – the domain where the investigation is done - consists of two lumbar vertebrae and the intervertebral disc between them. Afterwards, the tools of biomechanics and numerical analysis are availed; the computation is done within the finite element software. As we focus on the disc behavior, its changes, and vulnerability, the results are presented and discussed mainly on this part.

2 HUMAN SPINE ANATOMY

The human spine is a complex biological system within the organism. It consists of stiff vertebrae separated by elastic intervertebral discs. The particular parts of the spine differs each from other by the shape, composition; and there are some common features and functionality. That is why we speak about cervical part of the spine with 7 vertebrae (C1-C7), thoratic part with 12 vertebrae (T1-T12), lumbar part with 5 vertebrae (L1-L5), sacral part with 5 fused vertebrae (S1-S5), coccyges part with 4 or 5 fused vertebrae (Co1-Co4) or (Co1-Co5), see Fig.1. There are 23 intervertebral – within C1-L5 discs one by one between.

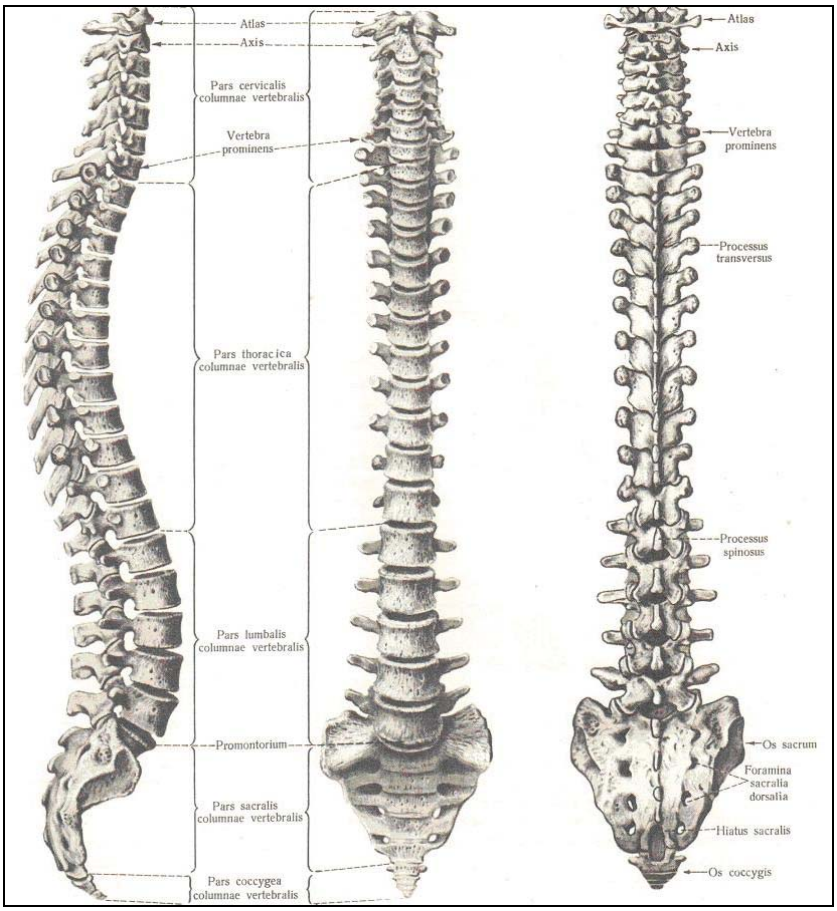

Fig. 1: Human spine; lateral view, anterior view, posterior view [6]

The vertebra consists of *vertebral body* – the essential load carrying part and the salients – *processi* joined to the body by strong *pedicles*. Among the vertebral body, pedicles and the salient there is a hole *foramen* – creating the spinal canal where the spinal cord leads through, see Fig.2a,b.

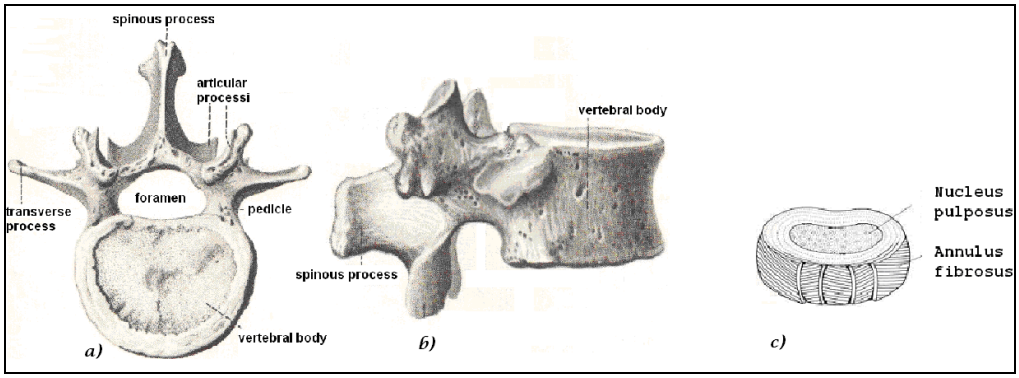

Fig. 2: Human spine; a) top view, b) lateral view, c) intervertebral disc sheme [6]

The intervertebral disc has three basic components. The inner part is *nucleus pulposus* – an almost incompressible liquid or jelly-like substance distributing hydraulic pressure in all directions within the disc, the outer part is created by the elastic layered *annulus fibrosus*. Its collagen content is divided to the layers by the system of fibers. The cartilage thin plate covering the disc at the bottom and at the top is called *endplate* [1], see Fig.2c.

3 BIOMECHANICS OF THE LUMBAR SPINE

Comparing to the other human vertebrae, the lumbar vertebrae have more robust bodies and pedicles and smaller processi. The shape is tailored to bearing about 60% of the body weight and to handle with all types of load.

3.1 Model simplification, coordinate system, notation

At the beginning of the intervertebral disc behavior within the lumbar motion segment, see Fig.3 we do some simplification. While dealing with a constraint, the main role is played by massive vertebral body of the lumbar motion segment. As proven by experiments, its concave part (top view see Fig.2.a) forming foramen hole does not play significant role while bearing the compressive load - the magnitude, but not the exact shape of the upper and lower surface is important while computing the stress – strain field. That is why it can be taken circular instead of oval shape during the investigation of the compression load impact to the intervertebral disc. Consequently using surface of revolution as the domain of the interest and taking uniform distributed load representing for example walking or jumping, the situation it can be investigated as axisymmetric. In the case of nonuniform distributed load the model is fully 3D, with cylindrical system of coordinates applied.

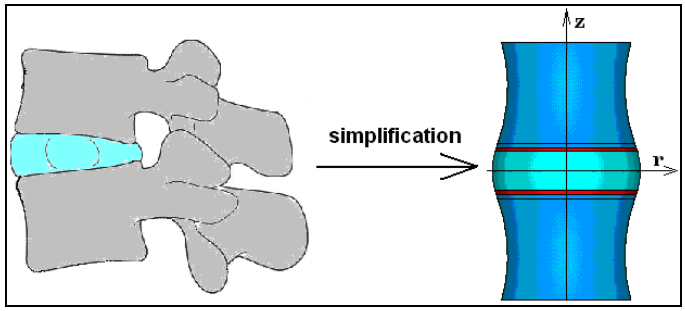

Fig. 3: Motion segment and its first approximation configuration[4]

Regarding that the domain of our interest is a surface of revolution, we use *cylindrical coordinate system (r, z, θ)*, see Fig.4., with ***r*** **-** *radial* coordinate (distance from the axis of the revolution, r ≥ 0), ***z*** **-** *axial* coordinate, and ***θ*** - *circumferential* coordinate.

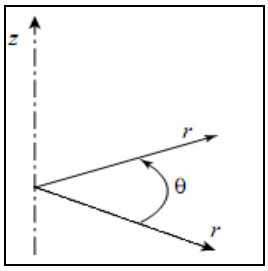

Fig. 4: The cylindrical coordinate system coordinates

The notation is

- *displacement field*

  in axisymmetric case (AXI)

$$\mathbf{u}(r,z)=\begin{bmatrix} u_r(r,z) \\ u_z(r,z) \end{bmatrix}$$

  in full 3D, cylindrical coordinate system (CYL)

$$\mathbf{u}(r,z,\theta)=\begin{bmatrix} u_r(r,z,\theta) \\ u_z(r,z,\theta) \\ u_\theta(r,z,\theta) \end{bmatrix}$$

- *strain* tensor

$$\mathbf{e}_{\mathbf{AXI}}=\begin{bmatrix} e_{rr} & e_{rz} & 0 \\ e_{rz} & e_{zz} & 0 \\ 0 & 0 & e_{\theta\theta} \end{bmatrix}, \text{ rearranged } \mathbf{e}_{\mathbf{AXI}}=\begin{bmatrix} e_{rr} \\ e_{zz} \\ e_{\theta\theta} \\ \gamma_{rz} \end{bmatrix}, \quad \mathbf{e}_{\mathbf{CYL}}=\begin{bmatrix} e_{rr} & e_{zr} & e_{\theta r} \\ e_{rz} & e_{zz} & e_{\theta z} \\ e_{r\theta} & e_{z\theta} & e_{\theta\theta} \end{bmatrix}, \text{ rearr. } \mathbf{e}_{\mathbf{CYL}}=\begin{bmatrix} e_{rr} \\ e_{zz} \\ e_{\theta\theta} \\ \gamma_{rz} \\ \gamma_{r\theta} \\ \gamma_{\theta z} \end{bmatrix}$$

  where $\gamma_{rz}=e_{rz}+e_{zr}=2e_{rz}$

$$\gamma_{r\theta}=e_{r\theta}+e_{\theta r}=2e_{r\theta}$$

$$\gamma_{\theta z}=e_{\theta z}+e_{z\theta}=2e_{\theta z}$$

- *stress* tensor

$$\boldsymbol{\sigma}_{\mathbf{AXI}}=\begin{bmatrix} \sigma_{rr} & \sigma_{rz} & 0 \\ \sigma_{rz} & \sigma_{zz} & 0 \\ 0 & 0 & \sigma_{\theta\theta} \end{bmatrix}, \text{ or } \boldsymbol{\sigma}_{\mathbf{AXI}}=\begin{bmatrix} \sigma_{rr} \\ \sigma_{zz} \\ \sigma_{\theta\theta} \\ \sigma_{rz} \end{bmatrix}, \quad \boldsymbol{\sigma}_{\mathbf{CYL}}=\begin{bmatrix} \sigma_{rr} & \sigma_{rz} & \sigma_{r\theta} \\ \sigma_{zr} & \sigma_{zz} & \sigma_{z\theta} \\ \sigma_{\theta r} & \sigma_{\theta z} & \sigma_{\theta\theta} \end{bmatrix}, \text{ or } \boldsymbol{\sigma}_{\mathbf{CYL}}=\begin{bmatrix} \sigma_{rr} \\ \sigma_{zz} \\ \sigma_{\theta\theta} \\ \sigma_{rz} \\ \sigma_{r\theta} \\ \sigma_{\theta z} \end{bmatrix}$$

  where $\sigma_{rz}\equiv\sigma_{zr},\sigma_{r\theta}\equiv\sigma_{\theta r},\sigma_{\theta z}\equiv\sigma_{z\theta}$

3.2 Mechanical laws in the biological system

In the two considered load types the axisymmetric or 3D approach is chosen

• *Kinematical equations* describe the strain-displacement relation:

$$\mathbf{e} = \mathbf{D}\mathbf{u}, \tag{3.1}$$

where in axisymmetric case $\mathbf{e} = \mathbf{e}_{AXI}$ and in cylindrical 3D case $\mathbf{e} = \mathbf{e}_{CYL}$ and

$$\mathbf{D}_{AXI} = \begin{bmatrix} \frac{\partial}{\partial r} & 0 \\ 0 & \frac{\partial}{\partial z} \\ \frac{1}{r} & 0 \\ \frac{\partial}{\partial z} & \frac{\partial}{\partial r} \end{bmatrix}, \qquad \mathbf{D}_{CYL} = \begin{bmatrix} \frac{\partial}{\partial r} & 0 & 0 \\ 0 & \frac{\partial}{\partial z} & 0 \\ \frac{1}{r} & 0 & \frac{1}{r}\frac{\partial}{\partial \theta} \\ \frac{\partial}{\partial z} & \frac{\partial}{\partial r} & 0 \\ \frac{1}{r}\frac{\partial}{\partial \theta} & 0 & \frac{\partial}{\partial r} - \frac{1}{r} \\ 0 & \frac{1}{r}\frac{\partial}{\partial \theta} & \frac{\partial}{\partial z} \end{bmatrix}.$$

• *Constitutive equations (Hooke's law)* express the dependence of the stress on the strain:

$$\boldsymbol{\sigma} = \mathbf{E}\,\mathbf{e} \tag{3.2}$$

The isotropic material, is characterized by unique elastic modulus E and Poisson's ratio ν the general constitutive equation can be rewritten in the form:

$$\mathbf{E}_{AXI} = \frac{E}{(1+\nu).(1-2\nu)} \begin{bmatrix} 1-\nu & \nu & \nu & 0 \\ \nu & 1-\nu & \nu & 0 \\ \nu & \nu & 1-\nu & 0 \\ 0 & 0 & 0 & \frac{1}{2}(1-2\nu) \end{bmatrix},$$

$$\mathbf{E}_{CYL} = \frac{E}{(1+\nu).(1-2\nu)} \begin{bmatrix} 1-\nu & \nu & \nu & 0 & 0 & 0 \\ \nu & 1-\nu & \nu & 0 & 0 & 0 \\ \nu & \nu & 1-\nu & 0 & 0 & 0 \\ 0 & 0 & 0 & \frac{1}{2}(1-2\nu) & 0 & 0 \\ 0 & 0 & 0 & 0 & \frac{1}{2}(1-2\nu) & 0 \\ 0 & 0 & 0 & 0 & 0 & \frac{1}{2}(1-2\nu) \end{bmatrix}$$

- *Equilibrium equations*, e.g.[3]

in axisymmetric case:

$$\begin{aligned} &\frac{1}{r}\frac{\partial}{\partial r}(r\sigma_{rr})+\frac{\partial}{\partial z}\sigma_{rz}-\frac{\sigma_{\theta\theta}}{r}+b_r=0\\ &\frac{1}{r}\frac{\partial}{\partial r}(r\sigma_{zr})+\frac{\partial}{\partial z}\sigma_{zz}+b_z=0\\ &b_{\theta\theta}=0, \end{aligned} \tag{3.3}$$

in full 3D; cylindrical coordinate system:

$$\begin{aligned} &\frac{1}{r}\frac{\partial}{\partial r}(r\sigma_{rr})+\frac{\partial}{\partial z}\sigma_{rz}-\frac{\sigma_{\theta\theta}}{r}+b_r=0\\ &\frac{1}{r}\frac{\partial}{\partial r}(r\sigma_{zr})+\frac{\partial}{\partial z}\sigma_{zz}+b_z=0\\ &\frac{1}{r^2}\frac{\partial}{\partial r}(r^2\sigma_{\theta r})+\frac{\partial}{\partial z}\sigma_{\theta z}+b_\theta=0, \end{aligned} \tag{3.4}$$

where b_r, b_z, b_θ are body force vector components.

3.3 Finite element modeling

Variation formulation is based on the *total potential energy functional* minimization. Taking displacements as master field, the total potential energy functional is of the form [5], [7]:

$$\Pi[\mathbf{u}] = \boldsymbol{U}[\mathbf{u}] - \boldsymbol{W}[\mathbf{u}], \tag{3.5}$$

where $\boldsymbol{U}[\mathbf{u}]$ is the strain energy functional,

$$\boldsymbol{U}[\mathbf{u}]=\frac{1}{2}\int_V \boldsymbol{\sigma}^T\mathbf{e}\,dV=\frac{1}{2}\int_V \mathbf{e}^T\mathbf{E}\mathbf{e}\,dV\,, \tag{3.6}$$

$\boldsymbol{W}[\mathbf{u}]$ is the external work potential that can be written as a sum of contributions due to body force and contributions due to prescribed surface tractions,

$$\boldsymbol{W}[\mathbf{u}] = \boldsymbol{W_b}[\mathbf{u}] + \boldsymbol{W_t}[\mathbf{u}], \tag{3.7}$$

where

$$\boldsymbol{W_b}[\mathbf{u}]=\int_V \mathbf{b}^T\mathbf{u}\,dV\,, \tag{3.8}$$

$$\boldsymbol{W_t}[\mathbf{u}]=\int_{S_t} \mathbf{t}^T\mathbf{u}\,dS\,. \tag{3.9}$$

In the case of axisymmetry, the element of volume dV in (3.8) can be taken as a "ring element" $dV = 2\pi r dA$, where dA is an element of cross sectional area, and the element of surface $dS = 2\pi r ds$ in (3.9), ds being arc length element. Thus the *strain energy functional in the case of rotation symmetry* is of the form

$$\boldsymbol{U}[\mathbf{u}]=\frac{1}{2}2\pi\int_A r\,\mathbf{e}^T\mathbf{E}\mathbf{e}\,dA \tag{3.10}$$

and external work potential of the form

$$\boldsymbol{W}[\mathbf{u}] = \boldsymbol{W_b}[\mathbf{u}] + \boldsymbol{W_t}[\mathbf{u}]= 2\pi\int_A r\,\mathbf{b}^T\mathbf{E}\mathbf{e}\,dA + 2\pi\int_{s_t} r\,\mathbf{t}^T\mathbf{u}\,ds \tag{3.11}$$

3.4 Input parameters and computing

• Boundary conditions

There are two types of load applied. For the sake of better synopsis in axisymmetric case the "zero level plane" (that the all computations are done relatively to) leads horizontally in the middle of the disc, just horizontal displacement is allowed on it. In fully 3D the plane containing the lower surface of the lower vertebra is considered as a pad. There all degrees of freedom of this point are detracted. In both types of load the upper surface is the place where the two various loads (p1, p2) one are applied.

p1: Uniform distributed load of 480N per the upper area

p2: Parameterized non-uniform distributed load given by a function. We take the linear function in two variables with Tmax and Tmin values on the opposite borders of the disc diameter.

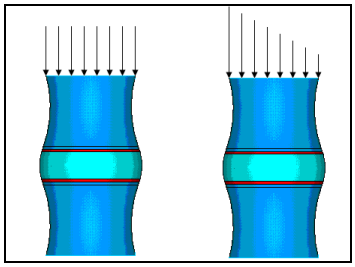

Fig. 5: Uniform and non – uniform distribution load

• Material properties

As mentioned in chapter 2, the vertebra consists of cortical and cancellous bone; the disc consists of annulus fibrosus and nucleus pulposus, see Fig.6. They are separated by cartilaginous endplate. All materials are supposed to be isotropic. The Young modulus and Poisson ratio constants are given in the table 1.

Tab. 1: Material properties of the biological system components [8]

	Cortical bone	Cancellous bone	Annulus fibrosus	Nucleus pulposus	Endplate
Young modulus [MPa]	12000	120	24.20	0.013	24.3
Poisson ratio [-]	0.3	0.2	0.4	0.499999	0.20

• Finite element type

The type of the element within the finite element software was chosen according to the type of the task and the required results.

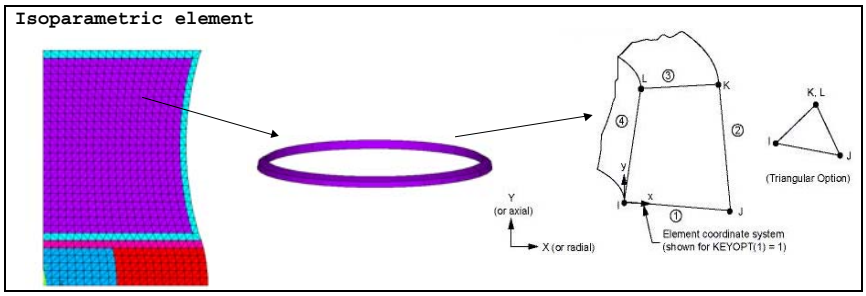

Fig. 6: Meshed area representing the simplified motion segment - body of revolution and its configuration; 2D element represents a ring in reality [2]

The linear 4-node plane element was used in the case of axisymmetry, Fig.6 and the higher order 3D 20-node solid element that exhibits quadratic displacement behavior was taken in fully 3D approach, Fig.7 [2].

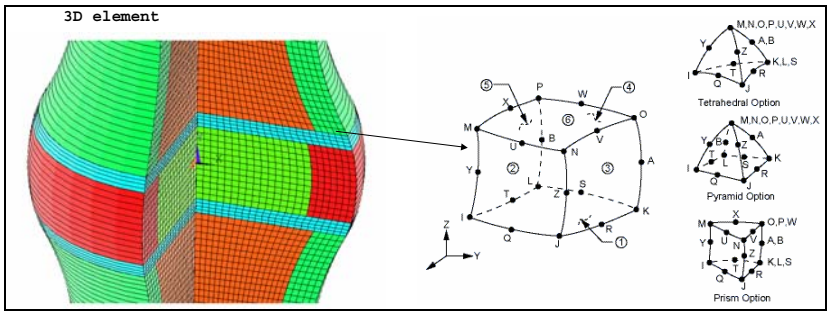

Fig. 7: Meshed body by higher order type of element while fully 3D approach is used

4 RESULTS

As all dimensions of all components of the model are parameterized, the geometry can vary and in such matter it is possible to predict the behavior of the several possible motion segments within the human spine.

We chose the L3 – L4 configuration, it means all indicated results correspond with the motion segment consisting of the 3rd and the 4th vertebrae of the human lumbar spine and appropriate intervertebral disc between them.

4.1 Uniform p1 load applied

The p1 load case is judged as fully axisymmetric, as the domain is a surface of revolution and the load is symmetric. Zero level (the plane that all displacements are computed relatively to) leads horizontally in the middle of the disc.

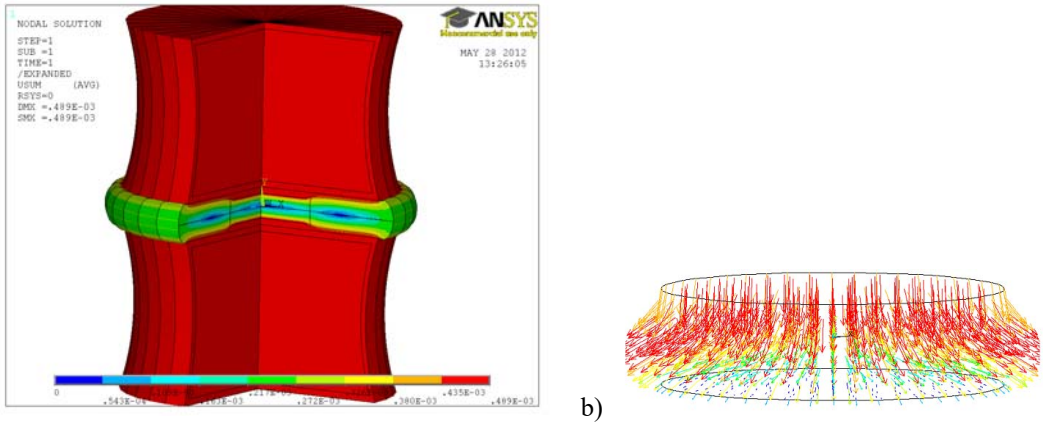

a) b)

Fig. 8: a) Motion segment under the p1 load; isosurfaces of displacements,
b) disc nodes displacement vectors under such a load

We can se on the Fig.8 and Fig.9, which the liquid inner part of the disc - nucleus pulposus changed its shape under the load and forced the elastic annulus fibrosus to deform outside radially. The deformations are of the magnitude about ½ mm at the point of the very outer circle of disc.

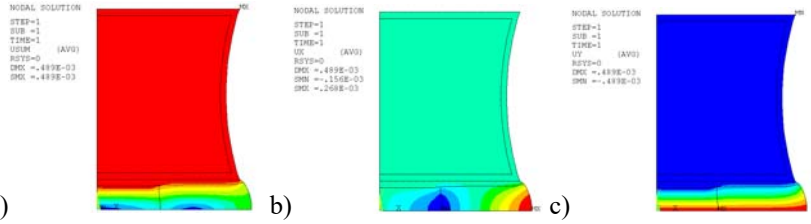

a) b) c)

Fig. 9: Displacement of motion segment nodes under the L1 load a) displacement magnitude, b) r-component of displacement, c) z-component of displacement

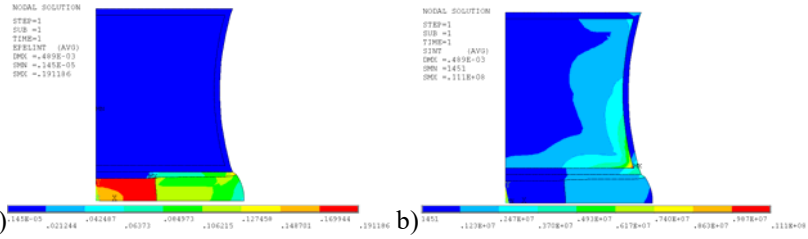

a) b)

Fig. 10: a) Strain, b) stress magnitude within the quarter of the motion segment

The maximal stress magnitude, Fig.10b), is observed in the bottom tip of the cancellous bone on the border with the cortical bone where the most deforming part of the disc is connected by its endplate. As expected, the strain, Fig.10a), gains its maximum in the liquid nucleus, that changes its shape easily. Also the deformation of the elastic annulus fibrosus is significant.

4.2 Non-uniform p2 load applied

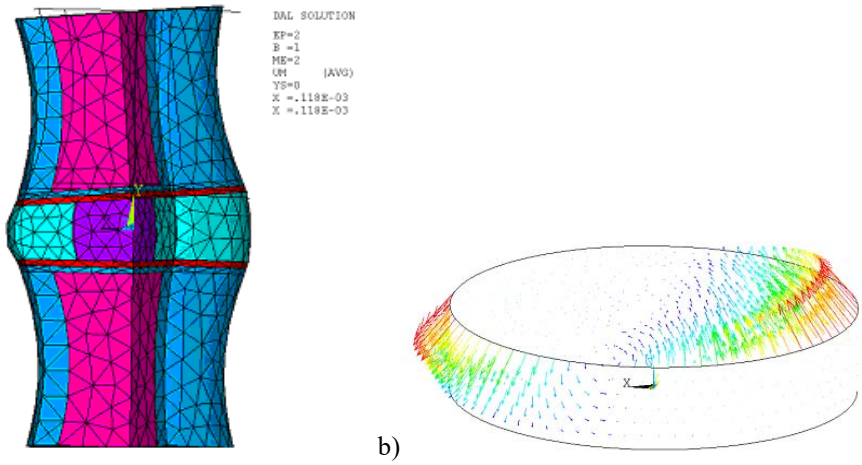

a) b)

Fig. 11: a) Deformation of the motion segment under the non-uniformed distributed load, b) displacement vectors of the nodes

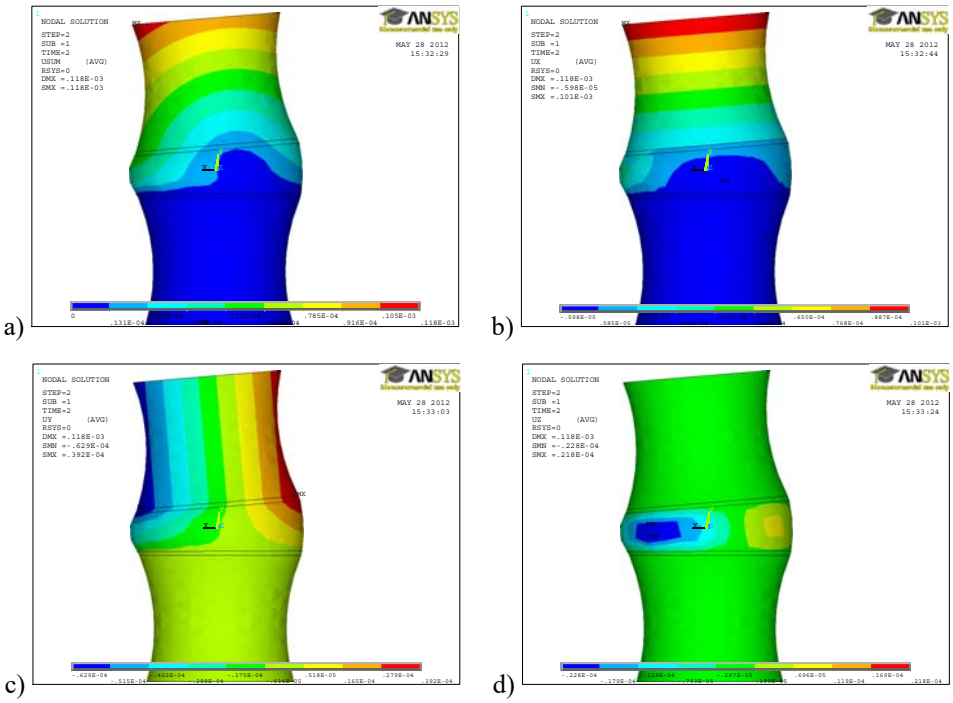

Fig. 12: Displacement isosurfaces under non – uniform distributed load a) magnitude of the total displacement, b) its x-component, c) y-component d) z-component

In the case of bending / extending the bottom area on the pad is considered as a zero level. The lower vertebra particles did not move at all, upper vertebra just moved, but did not deform at all, just the elastic disc deform significantly.

5 CONCLUSION

The stress – strain response of the human spine segment under the various types of physiological load reminds the orthopaedist the places with the concentrated stress which can lead to the disc herniation under the overloading. The parametrizing of the dimensions makes the model universal for several motion segment of human lumbar spine. Problem of the mechanical response of the particular parts of the human lumbar spine is complex, still not observed sufficiently. Therefore further we will aim to more complex models by detailing of the intervertebral disc composition, including nonlinear physical properties, adding the ligaments into the model, etc.

ACKNOWLEDGEMENT

This work is supported by grant APVV 0351-07.

REFERENCES

[1] ADAMS, M., BOGDUK, N., BURTON, P., DOLAN, P., (1979): The Biomechanics of Back Pain. Edinburgh, London, New York, Philadelphia, St Louis, Toronto; Churchill Livingstone, intervertebral discs. J. Biomech. Vol. 12, pp. 453 - 458.

[2] ANSYS help

[3] MINÁROVÁ M., SUMEC J., (2012): Mechanics of lumbar part of the human spine, mathematical model and computations; Acta of Bioengineering and Biomechanics, Publisher: Wroclaw University of Technology, Poland. (In press)

[4] PANJABI, M.M. et al., (1992): Human Lumbar vertebrae Quantitative Three Dimencional Anatomy, Spine, Vol.17, No.3, pp. 299 – 306.

[5] REDDY, J., (1993): An introduction to the Finite Element, McGraw-Hill, New York, ISBN 0-07-112799-2.

[6] SINELNIKOV, R.D., (1980): Atlas anatomie člověka, I. díl, AVICENUM – zdravotnické nakladatelství Praha (in Czech language).

[7] SPILKER, R.L:, (1982): A Simpilfied Hybrid-stress Finite Element Model of the Intervertebral Disc, Finite Elements in Biomechanics, University of Arizona, 14 chapter.

[8] VALENTA, J. (1985): Biomechanika, Academia, ,1.vyd., 539 p., ISBN 80-246-0306

Reviewers:

Prof. Ing. Josef Jíra, CSc., Department of Mechanics and Materials, Faculty of Transportation Sciences, Czech Technical University in Prague.

Doc. Ing. Eva Kormaníková, PhD., Department of Structural Mechanics, Faculty of Civil Engineering, Technical University of Košice.